

## The interplay between *Dendrobium Officinale* polysaccharide, gut microbiota, and lipid metabolism in HFD/STZ-induced type 2 diabetic mice

Muthukumaran Jayachandran\*, Jia Liu, Shen Qu\*

Department of Endocrinology and Metabolism, Shanghai Tenth People's Hospital, School of Medicine, Tongji University, Shanghai 200072, China

\*Corresponding Authors: Muthukumaran Jayachandran and Shen Qu, Department of Endocrinology and Metabolism, Shanghai Tenth People's Hospital, School of Medicine, Tongji University, No. 301 Middle Yanchang Road, Shanghai, 200072, China. Emails: [qushencn@hotmail.com](mailto:qushencn@hotmail.com); [19310210@tongji.edu.cn](mailto:19310210@tongji.edu.cn)

Academic Editor: Prof. Tommaso Beccari, University of Perugia, Italy

Received: 3 April 2025; Accepted: 31 July 2025; Published: 1 January 2026

© 2026 Codon Publications

OPEN ACCESS 

RESEARCH

### Abstract

Dietary polysaccharides are effective in mitigating hyperglycemia, insulin resistance, and improving the condition of people with type 2 diabetes mellitus (T2DM). Our investigation explored the changes in the normal microbiome that occur upon high-fat diet feeding and how dietary *Dendrobium officinale* polysaccharides (DOP) can benefit the treatment of T2DM by mitigating gut microbial dysbiosis. In addition, we have evaluated the changes in lipid metabolism in T2DM mice. Results suggest that HFD feeding (8 weeks) and streptozotocin (120 mg/kg b.w) result in insulin resistance, hyperlipidemia, and gut microbial dysbiosis associated with T2DM. Treatment with DOP results in improved glucose and insulin tolerance, as well as a better plasma and tissue lipid profile. In addition, histopathological and molecular changes support the biochemical observations. Results of gut microbiome studies based on 16S rRNA sequencing suggest that DOP plays a role in improving the population of beneficial bacterial species. In summary, DOP attenuated hyperlipidemia by regulating gut microbial dysbiosis in T2DM.

**Keywords:** Dietary polysaccharides; *Firmicutes/Bacteroidetes*; Gut microbial dysbiosis; Insulin resistance; Type 2 diabetes mellitus.

### Introduction

The global predominance of diabetes mellitus in adults (aged 20 to 79) is projected to be 10.5%, affecting roughly 530 million people worldwide (Sun *et al.*, 2022). In particular, type 2 diabetes mellitus (T2DM) is considered a potential health concern affecting people from different regions. T2DM impacts an individual's everyday functions and quality of life, and in the worst-case scenario, leads to death. The aspects that contribute to the onset and progression of T2DM vary, including changes in dietary habits, high basal metabolic index (BMI), tobacco

use, alcohol consumption, and a lack of physical activity (Kheriji *et al.*, 2023). An unhealthy dietary habit can lead to a high BMI and obesity, which in turn increases the risk of developing insulin resistance in various tissues and T2DM (Ruze *et al.*, 2023). Upon obesity, adipose tissue releases multiple hormones, pro-inflammatory cytokines, fatty acids, and other factors contributing to insulin resistance (Wondmkun, 2020). The oversecretion of insulin by beta cells in response to insulin resistance and hyperglycemia results in the failure of beta cells. Hence, hyperglycemia, insulin resistance, and beta-cell dysfunction are the key factors to be studied in T2DM.

The treatment methods for T2DM include a healthy diet, changes in physical activities, oral antidiabetic medications (sulfonylureas, meglitinides, thiazolidinediones,  $\alpha$ -glucosidase inhibitors, DPP IV inhibitors, etc.), and bariatric surgery (laparoscopic sleeve gastrectomy, Roux-en-Y gastric bypass, and adjustable gastric banding) (Chong *et al.*, 2024).

Although the treatment methods mentioned above provide significant improvement in T2DM management, interest in dietary-mediated changes in T2DM pathology has garnered much attention because of their ease of accessibility and lack of harmful effects. In our previous studies, we have demonstrated the antidiabetic efficacy of various dietary phytochemicals and polysaccharides, as well as their ability to regulate gut microbial populations beneficially (Jayachandran *et al.*, 2019; Jayachandran *et al.*, 2020; Jayachandran *et al.*, 2023; Li *et al.*, 2021; Zhao *et al.*, 2020). Through modulation of gut microbiota diversity, dietary polysaccharides can exhibit prebiotic-like properties, potentially treating T2DM (Cunningham *et al.*, 2021). This was demonstrated in our previous study on dietary polysaccharide Konjac glucomannan, which exhibited antioxidant, anti-inflammatory, antihyperlipidemic, and antidiabetic efficacy (Li *et al.*, 2021; Zhao *et al.*, 2020). In addition, KGM significantly regulates the beneficial bacterial flora in the gut, thereby improving gut health and T2DM (Jayachandran *et al.*, 2023). Similarly, in this study, we postulate the investigation of the outcomes of DOP on T2DM mice.

DOP is a biologically active polysaccharide extracted from *Dendrobium officinale* and used as a potential herbal medicine in traditional Chinese medicine (Liu *et al.*, 2020). DOPs are water-soluble, non-starchy polysaccharides that constitute approximately 20% of the total extract (Wu *et al.*, 2023). Studies indicate that the major composition of DOP consists of 1,4- $\beta$ -D-glucose, 1,4- $\beta$ -D-mannose, and O-acetate groups (Liu *et al.*, 2023). Research from other groups and our preliminary study has indicated that DOP possesses several health-benefiting properties, including antioxidant, anti-inflammatory, antidiabetic, immunomodulatory, and anticancer effects (Xu *et al.*, 2022). Notable studies have found that DOPs are resistant to regular digestion processes, and actual metabolism occurs in the large intestine through gut microbes (Li *et al.*, 2019). This gut microbial-mediated metabolism of DOPs yields oligosaccharides and various short-chain fatty acids (SCFAs). These metabolic products are recognized for their role in regulating gut microbiota and for enhancing overall health. A decline in harmful gut bacterial flora, including *Escherichia* and *Staphylococcus*, and an increase in beneficial bacterial flora, such as *Bacteroides*, *Bifidobacterium*, *Lactobacillus*, *Akkermansia*, and *Prevotella*, are the primary reasons that could make

the DOP a potential prebiotic in disease intervention (Wu *et al.*, 2023).

Although numerous studies have studied the potential health benefits of DOP in experimental animals, research on its antihyperlipidemic effects in the context of gut microbial regulation, with evidence from molecular pathway changes, is lacking. Hence, we have designed this experiment to explore the antihyperlipidemic effects of DOP on HFD/STZ-induced T2DM mice. Furthermore, we planned to examine the changes in gut microbial dysbiosis that favor the management of T2DM. The final results of this experiment could aid in categorizing the prebiotic role of DOP in regulating the gut microbial population and provide a more effective treatment strategy for preventing T2DM.

## Experimental Materials and Methods

### Polysaccharides and general chemicals

DOP was purchased from Baicao Organism, China. Key chemicals, such as streptozotocin (STZ) and pioglitazone (PIO), were purchased from Sigma-Aldrich, Shanghai, China. The general chemicals were acquired from Shanghai Macklin Biochemical Co., Ltd. (Shanghai, China).

### General characteristics and acclimatization of mice

The male C57BL/6N mice (n=24) with healthy conditions (20 g to 25 g) and normal glucose levels were used for this study. The 6- to 8-week-old mice were procured from the Shanghai Model Organisms Center, Inc., Shanghai, China. The experimental animal house of Shanghai Tenth People's Hospital was utilized to access pathogen-free polypropylene cages, which were obtained with prior permission to perform the animal study, in accordance with the guidelines of the ethical committee (SHDSYY-2023-1981). Throughout the experimental period, the mice were given unlimited access to water and food. The National Institute of Health animal usage protocol was strictly adhered to. Before the actual experiments, we acclimated the mice for 2 weeks.

### T2DM induction and experimental grouping

Following a previous study, we have developed a mouse model (Male C57BL/6N mice) of T2DM (HFD+STZ) (Wang *et al.*, 2021). A high-fat diet (HFD) was purchased from Open-Source Diets, Research Diets, New Brunswick, NJ, USA, and its composition is as follows: 5.24 kcal/g, 60% kcal (fat), 20% kcal (carbohydrates), and 20% kcal (protein). The experimental animals were

divided into four groups. Group 1: control mice fed with a standard pellet diet throughout the experimental period. Group 2: diabetic mice fed with HFD throughout the experimental period and given STZ (120 mg/kg b.w) one time after 8 weeks of HF feeding. Group 3: diabetic mice fed with HFD (8 weeks)/STZ and treated with DOP (80 mg/kg b.w) (28 days). Group 4: diabetic mice fed with HFD (8 weeks)/STZ and treated with PIO (10µg/kg b.w) (28 days). The dose of DOP (80 mg/kg b.w) was determined based on preliminary studies (data not shown). Diabetic mice, defined by fasting blood glucose levels greater than 300 mg/dL, were included in the study.

### **Animal dissection and sample preservation**

Once the experimental procedure was completed, mice were kept fasting overnight. We have used chloral hydrate (24 mg/kg b.w) to anesthetize the mice and killed them by cervical decapitation.

### **Blood and tissue sample collection**

Using heparinized tubes, fresh blood samples were obtained from each animal, and the plasma was then obtained. Tissue samples were washed (saline) thoroughly to remove the blood stains and stored at -80 °C for molecular assays. Fresh tissue samples were homogenized and used for biochemical assays.

### **Tissue homogenate preparation**

Lipid extraction from mouse tissues was performed using the Folch *et al.* (1957) protocol. Tissues were rinsed with ice-cold saline and then homogenized in a chloroform: methanol mixture (2:1, v/v). After 24 hours at RT, the extraction was repeated four times. The pooled extracts were washed with 0.7% potassium chloride, and the upper aqueous layer was removed. The organic phase was collected, and chloroform was evaporated before lipid analysis.

### **Collection of fecal sample for 16S rRNA sequencing**

After overnight fasting, fecal samples were gathered in a sterile container. The collected samples were stored at -80 °C prior to the experiments.

### **Oral glucose tolerance test (OGTT)**

An OGTT was conducted according to the earlier procedures described by Du Vigneaud and Karr (1925).

Animals were fasted overnight to prepare for the test, the blood of mice was collected at "0" minute, and blood glucose levels were noted. Furthermore, a glucose solution (2 g/kg body weight) was administered, and glucose levels were monitored at defined time points (0, 30, 60, 90, and 120 minutes) using an Accu-Chek glucometer (Roche Diagnostics, Mannheim, Germany).

### **Insulin tolerance test (ITT)**

Similar to OGTT, animals were kept fasting overnight before the ITT, blood glucose values were noted at "0" minute, and mice were given an insulin injection (1-1.2 units/kg) intraperitoneally. The insulin doses were measured based on the weight of the different mice. Post-injection, glucose levels were measured using the Accu-Chek Glucometer at the following time intervals: 0, 30, 60, 90, and 120 minutes.

### **Plasma and tissue lipid profile**

The lipid profile diagnosis kit (Nanjing Jiancheng Bioengineering Institute, Nanjing, China) was used to analyze plasma total cholesterol (TC), triglycerides (TG), high-density lipoprotein (HDL), and low-density lipoprotein (LDL). Very low-density lipoprotein (VLDL) was measured as TG divided by 5. We have analyzed the TC and TG in the liver homogenate.

### **Histopathological analyses**

#### *H and E staining of liver and adipose tissue*

Liver and adipose tissues were used for performing H&E staining. After dissection, the respective tissue samples were fixed in 10% formalin. 5 mm-thick tissue segments were made from paraffin-embedded tissue blocks. The slides were then stained with hematoxylin and eosin as per standard procedure, and images were captured at 200x magnification.

#### *Oil red O staining of the liver*

The liver sections (frozen) were cut at 8 to 10 mm and then air-dried. The dried slides were then fixed in a formalin solution. Followed by washing for 1-10 minutes with running tap water. Rinse the slides with 60% isopropanol, and then stain the slides with Oil Red O solution (prepared at the time of the experiment) for 15 minutes. Once the incubation time is complete, rinse the slides with 60% isopropanol and stain them with alum hematoxylin (approximately 5 dips). Finally, rinse the stained slides with water and mount the slides with an aqueous mount and coverslip.

## Gene sequencing analyses

### Extraction of DNA and PCR amplification

Total microbial genomic DNA was extracted from fecal samples using the E.Z.N.A.<sup>®</sup> Soil DNA Kit (Omega Bio-Tek, Norcross, GA, USA) following the manufacturer's instructions. The DNA samples were stored at  $-80^{\circ}\text{C}$  prior to the experiments. The concentrations of the DNA samples were assessed using the NanoDrop<sup>®</sup> ND-2000 spectrophotometer (Thermo Scientific Inc., USA). The V3–V4 hypervariable region of the bacterial 16S rRNA gene was amplified using the primer pair 338F (5'-ACTCCTACGGGAGGCAGCAG-3') and 806R (5'-GGACTACHVGGGTWTCTAAT-3') on an ABI GeneAmp<sup>®</sup> 9700 PCR thermocycler (ABI, CA, USA), as previously described by Liu *et al.* (2016). The composition of the PCR mixture is as follows: Each 20  $\mu\text{L}$  PCR reaction mixture contained 10 ng of template DNA, 4  $\mu\text{L}$  of 5 $\times$  FastPfu buffer, 2  $\mu\text{L}$  of 2.5 mM dNTPs, 0.8  $\mu\text{L}$  each of forward and reverse primers (5  $\mu\text{M}$ ), 0.4  $\mu\text{L}$  of FastPfu DNA polymerase, and nuclease-free water (ddH<sub>2</sub>O) to adjust the final volume. The amplification settings are as follows: 1. Denaturation at 95  $^{\circ}\text{C}$  for 3 min, 2. Denaturing at 95  $^{\circ}\text{C}$  for 30 s (27 cycles), 3. annealing at 55  $^{\circ}\text{C}$  for 30 s, 4. extending at 72  $^{\circ}\text{C}$  for 45 s, 5. The extension was performed at 72  $^{\circ}\text{C}$  for 10 minutes, followed by a cooling step to 4  $^{\circ}\text{C}$ . The Triplicate of each sample was utilized for the amplification. Using 2% agarose gel. The final PCR product was separated on a 2% agarose gel, refined using the AxyPrep DNA Gel Extraction Kit (Axygen Biosciences, Union City, CA, USA), and quantified using the Quantus<sup>TM</sup> Fluorometer (Promega, USA).

### Illumina MiSeq sequencing

Majorbio Bio-Pharm Technology Co., Ltd. (Shanghai, China) has merged purified amplicons in equimolar proportions and executed paired-end sequencing on an Illumina MiSeq PE300 platform or NovaSeq PE250 platform (Illumina, San Diego, USA), following established methods. The NCBI Sequence Read Archive (SRA) database now holds the raw sequencing reads.

## Bioinformatics

Raw paired-end reads were quality-filtered using Fastp (v0.19.6) (Chen *et al.*, 2018) and subsequently merged with FLASH (v1.2.7) (Magoc and Salzberg, 2011). Trimming was performed at positions where the average quality score within a 50 bp sliding window fell below 20. Reads shorter than 50 bp or containing ambiguous nucleotides were removed from further analysis. Merged reads with  $\geq 10$  bp overlap and  $\leq 0.2$  mismatch rate were retained. High-quality reads were clustered into Operational Taxonomic Units (OTUs) at 97% similarity using UPARSE (v7.1) (Edgar, 2013). For each OTU, the

sequence with the highest abundance was selected to represent the cluster and classified taxonomically using the RDP Classifier (version 2.2) (Wang *et al.*, 2007) against the SILVA 16S rRNA database (version 138) (Quast *et al.*, 2013) with a confidence threshold of 0.7.

Functional prediction of microbial communities was performed using PICRUSt2 (Douglas *et al.*, 2020) based on representative OTU sequences. The pipeline utilizes HMMER, EPA-NG, Gappa, Castor, and MinPath to assign sequences to a reference tree, normalize gene copy numbers, and predict gene family and pathway abundances. Microbial community composition was profiled at both the phylum and genus levels. A community heatmap and cladogram were generated to visualize taxonomic differences, and the Microbial Dysbiosis Index (MDI) (Gevers *et al.*, 2014) was calculated to evaluate imbalance in microbial profiles. Data analyses were carried out on the Majorbio Cloud Platform (<https://cloud.majorbio.com>).

## Statistical analyses

One-way and two-way analysis of variance (ANOVA) and multiple comparisons among different groups were calculated using GraphPad Prism 8.0.2. The mean  $\pm$  standard deviation (S.D.) indicates the entire data set of total mice. The  $p < 0.0001$  signifies a considerable difference in statistical analysis between different groups. A bioinformatics study of the gut microbiota was performed via the Majorbio Cloud platform.

Alpha diversity indices, including Shannon index and Chao1 richness, were analyzed using Mothur (v1.30.1) (Schloss *et al.*, 2009). Differences between groups were assessed using the Kruskal–Wallis H test. Beta diversity was evaluated based on Bray–Curtis dissimilarity and visualized using Principal Coordinates Analysis (PCoA) at the OTU level and hierarchical clustering at the species level, both implemented via the Vegan package (v2.5-3) in R.

## Results

### Effect of DOP on OGTT

A regular test to check the body's capability to handle a glucose load is the OGTT. The control group (group 1) exhibited a gradual increase until 30 minutes, after which it started to decline. The diabetic group (group 2) showed a rise from 30 min and maintained this rise, without a considerable decline, even at 120 min. Conversely, upon treatment with DOP (80 mg/kg b.w.), the mice showed a considerable decrease after a peak at 30 minutes.

A comparable outcome was achieved in treatment with PIO (10 g/kg b.w.) (Figure 1A).

### Effect of DOP on ITT

The ITT is a basic screening test used to evaluate insulin action in patients with diabetes and assess insulin resistance. Our results suggest that the control group (Group 1) exhibits a gradual increase until 30 minutes, followed by a decline up to 120 minutes. The diabetic group (group 2) showed a rise from 30 minutes and

maintained this rise, without a considerable decline, even at 120 minutes. However, upon treatment with DOP (80 mg/kg b.w), the mice showed a considerable decrease, reaching a peak at 30 minutes. A-like effect was attained in mice given PIO (10 µg/kg b.w) (Figure 1B).

### Effect of DOP on plasma lipid profile

Dyslipidemia raises the risk of cardiovascular disease in diabetes mellitus. Figure 2 exhibits the plasma lipid profile (TC, TG, LDL, HDL, and VLDL). Diabetic mice

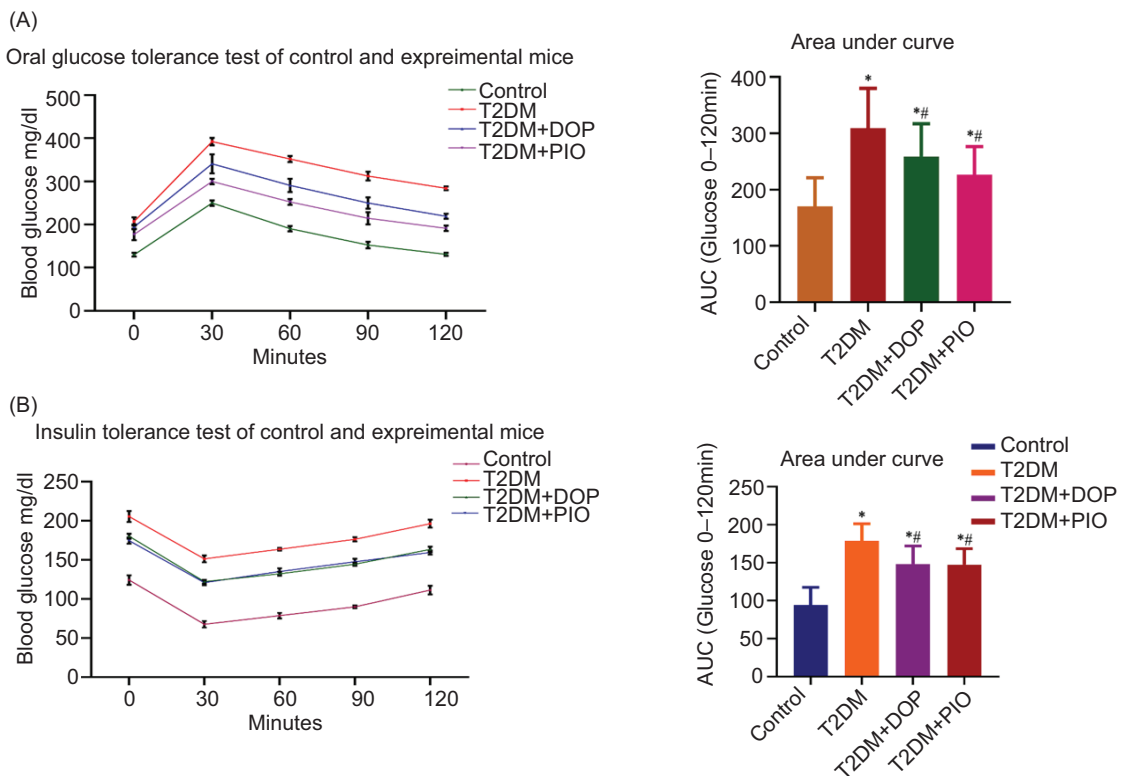


**Figure 1.** This figure illustrates the glucose and insulin tolerance tests performed. (A) Oral glucose tolerance test of control and experimental mice. Values were given as means ± S.D. for three mice in each group. At the time point “0” minutes, a significant difference of <0.0001 (\*\*\*\*) was observed in Control vs T2DM and Control vs T2DM+DOP. A significant difference of 0.0008 (\*\*\*) was observed between the Control and T2DM+PIO groups. A significant difference of 0.0067 (\*\*) was observed between T2DM and T2DM+PIO. No significant difference was observed between T2DM and T2DM+DOP, or between T2DM+DOP and T2DM+PIO. At the time point “30” minutes, a significant difference of <0.0001 (\*\*\*\*) was seen in control vs T2DM, Control vs T2DM+PIO, and T2DM vs T2DM+PIO. There was a significant difference of 0.0004 (\*\*\*) in Control vs T2DM+DOP, 0.0062 (\*\*) in T2DM vs T2DM+DOP, and 0.0206 (\*) in T2DM+DOP vs T2DM+PIO. At the time point “60” minutes, a significant difference of <0.0001 (\*\*\*\*) was observed in Control vs T2DM, Control vs T2DM+DOP, Control vs T2DM+PIO, and T2DM vs T2DM+PIO. A significant difference of 0.0002 (\*\*\*) was observed between T2DM and T2DM+DOP, and 0.0040 (\*\*) between T2DM+DOP and T2DM+PIO. At the time point “90” minutes, a significant difference of <0.0001 (\*\*\*\*) was seen in all comparisons except T2DM+DOP vs T2DM+PIO (0.0055). At the time point “120” minutes, a significant difference of <0.0001 (\*\*\*\*) was seen in all the comparisons. (B) Insulin tolerance test of control and experimental mice. Values were given as means ± S.D. for three mice in each group. At the time point “0” minutes, a significant difference of <0.0001 (\*\*\*\*) was seen between the control vs T2DM, Control vs T2DM+DOP, Control vs T2DM+PIO, and T2DM vs T2DM+PIO. A significant difference of 0.0004 (\*\*\*) was observed between T2DM and T2DM+DOP. There was no significant difference between T2DM+DOP vs T2DM+PIO. At the time point “30” minutes, a significant difference of <0.0001 (\*\*\*\*) was observed among all comparisons except the T2DM+DOP vs T2DM+PIO (No significance). A similar pattern was seen at time points 60, 90, and 120.

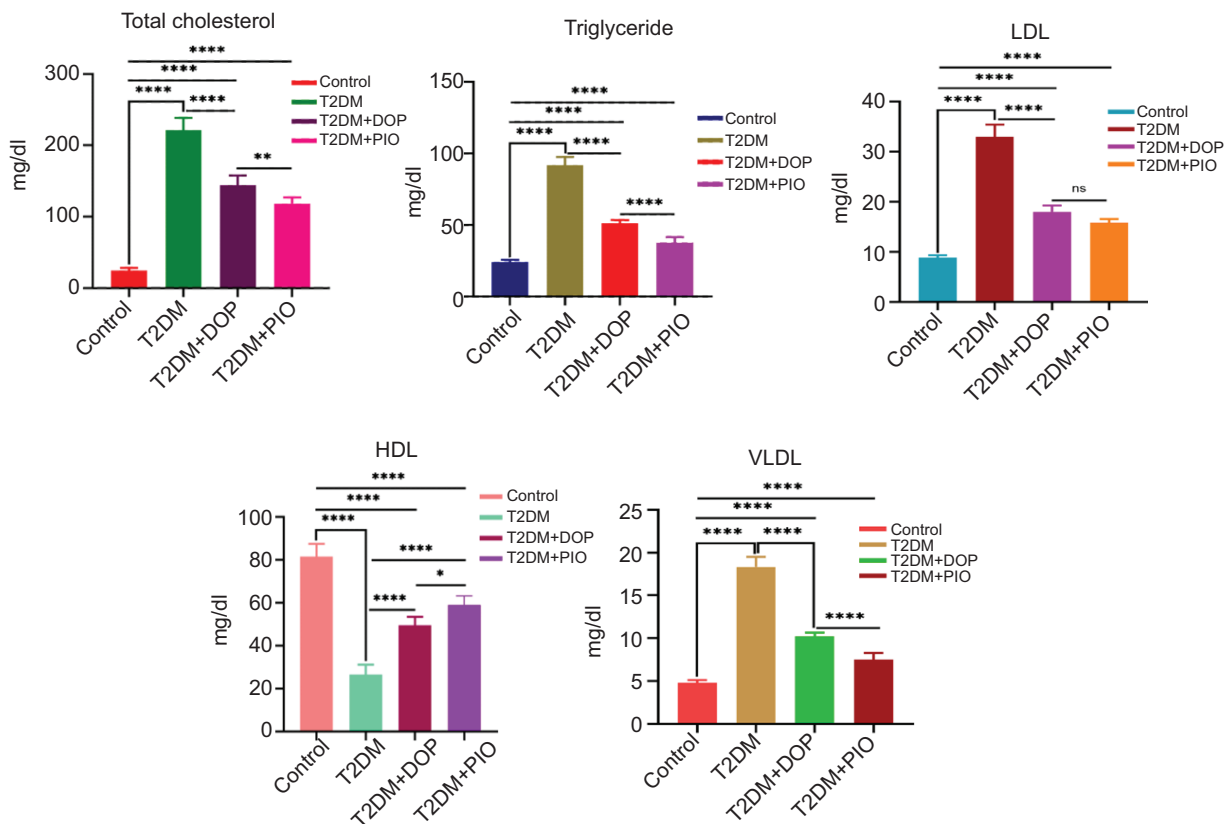


**Figure 2.** This figure depicts the plasma lipid levels in different experimental groups. The statistical difference <math><0.0001</math> (\*\*\*\*) indicates a significant difference among the groups. The groups with a statistical difference (\*\*) with a p-value (0.00691) in total cholesterol (T2DM+DOP vs T2DM+PIO), a statistical difference (\*) with a p-value (0.0118) in HDL (T2DM+DOP vs T2DM+PIO), and no significant difference in LDL (T2DM+DOP vs T2DM+PIO) were noted.

exhibit significantly elevated plasma lipid levels (TC, TG, LDL, and VLDL) compared to control mice ( $p < 0.0001$ ). Meanwhile, diabetic mice treated with DOP (80 mg/kg b.w) showed a decrease in the concentrations of plasma lipids (TC, TG, LDL, and VLDL). The results are comparable to those of diabetic mice given PIO (10  $\mu$ g/kg b.w). Meanwhile, HDL levels were decreased in diabetic mice and increased upon treatment with DOP (80 mg/kg b.w.) and PIO (10  $\mu$ g/kg b.w.).

**Effect of DOP on tissue lipid profile**

Figure 3 illustrates the TC and TG levels in the liver of experimental mice. Control mice show normal TC and TG levels. Meanwhile, diabetic mice show a substantial ( $p < 0.0001$ ) increase in TC and TG compared to control mice. The diabetic mice treated with DOP (80 mg/kg b.w) have shown a significant ( $p < 0.0001$ ) decrease in liver TC and TG. Similar results were achieved in diabetic mice treated with PIO (10  $\mu$ g/kg b.w).

**Effect of DOP on tissue morphology**

*Hematoxylin and eosin staining of liver and adipose tissue*

Hematoxylin and eosin staining helps identify alterations in the structure of cellular components, aiding in the differentiation between healthy and diseased conditions. Control mice show regular hepatic cells with clear nuclei. Diabetic mice show inflammatory infiltrations, lipid accumulation, and necrosis. The treatment of diabetic mice with DOP (80 mg/kg b.w) and PIO (10  $\mu$ g/kg b.w) has reduced inflammatory infiltrations, lipid accumulation, and necrosis in the liver.

Similar to the liver, adipose tissue shows changes in different groups. Control mice show normal adipocytes of regular size. Diabetic mice showed that the size of adipocytes was increased comparatively to control mice. Diabetic mice fed with DOP (80 mg/kg b.w.) exhibit anti-obesity effects through decreased adipocyte size. A similar change in size was seen in diabetic mice treated with PIO (10  $\mu$ g/kg b.w) (Figure 4A).

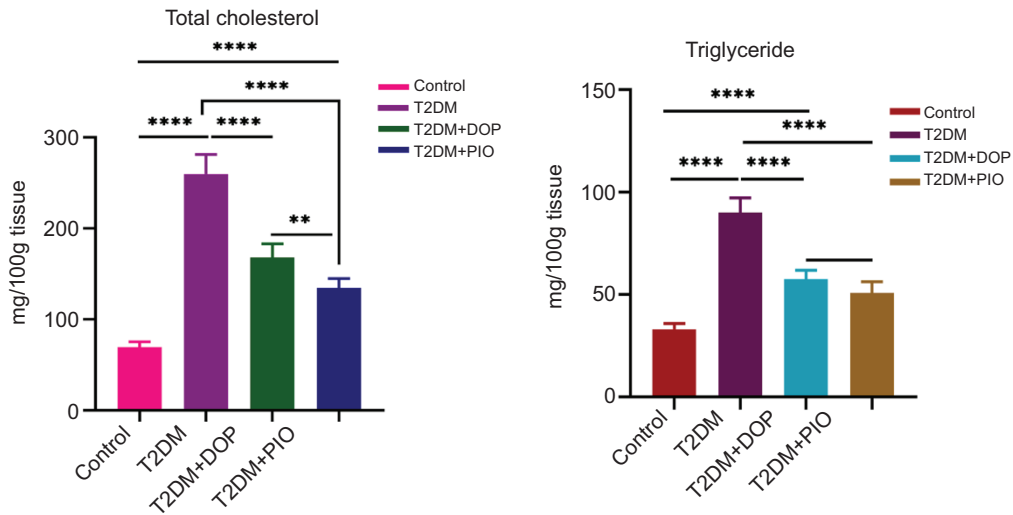


**Figure 3.** This figure illustrates the total cholesterol and triglyceride levels in the liver tissue of experimental mice. The statistical difference  $<0.0001$  (\*\*\*\*) indicates a significant difference among the groups. The groups with statistical significance (\*\*) with a p-value of 0.0032 in total cholesterol (T2DM+DOP vs T2DM+PIO) and no statistical significance in triglyceride (T2DM+DOP vs T2DM+PIO) were noted.

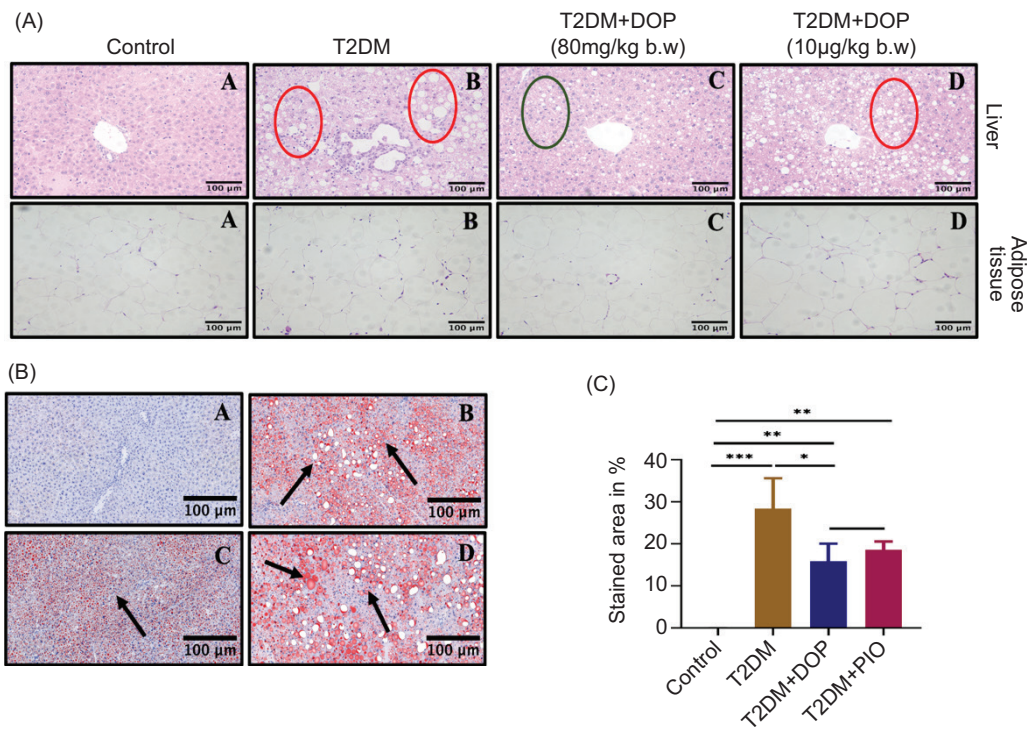


**Figure 4.** This figure illustrates the histopathological changes in the liver and adipose tissue of control and experimental mice. (A) Hematoxylin and eosin staining of the liver and adipose tissue (20 $\times$ ). (B) Oil red O staining of the liver (10 $\times$ ). (C) Quantification of stained area in Oil red O staining. Values were given as means  $\pm$  S.D. for three mice in each group. \*\*\*indicates the significant difference with p-value 0.0002 (Control vs T2DM), \*\*indicates the significant difference with p-value 0.0090 (Control vs T2DM+DOP), \*\*indicates the significant difference with p-value 0.0035 (Control vs T2DM+PIO), \*indicates the significant difference with p-value 0.0306, and ns indicates no significant difference among the groups.

**Oil red O staining of the liver**

The lipid substances in cells and tissues are identified efficiently using the special staining method Oil Red O. Figure 4B shows the Oil Red O staining in the liver of control and experimental mice. The control mice illustrate a regular liver histology with no hepatic lipid accumulation. In contrast, the diabetic group exhibits increased hepatic lipid accumulation, as indicated by the presence of red-stained lipid droplets throughout the liver. The diabetic mice treated with DOP (80 mg/kg b.w.) have shown an anti-obesity effect by reducing hepatic lipid accumulation and improving tissue morphology. Similar treatment effects were achieved in diabetic mice treated with PIO (10 µg/kg b.w.).

**Effect of DOP on fecal microbiota**

**Effect of DOP on alpha diversity**

The diversity found inside a particular area or ecosystem is referred to as alpha diversity. Metrics like coverage, ACE, Shannon, Chao, and Simpson are frequently employed. Our study results suggest that diabetic mice exhibit greater microbial diversity compared to control mice. Similarly, diabetic mice treated with DOP (80 mg/kg b.w.) exhibited significant changes in the microbial population, compared to diabetic mice (Figure 5A).

**Effect of DOP on beta diversity**

The variation in microbial composition between samples is known as beta diversity. Sample hierarchical clustering, sample distance heatmap graph, PCA analysis, PCoA analysis, NMDS analysis, NCM analysis, and ANOISM analysis are the methods to study beta diversity. Our results indicate that diabetic mice exhibit substantial differences in beta diversity compared to control mice. Meanwhile, diabetic mice treated with DOP (80 mg/kg b.w.) and PIO (10 µg/kg b.w.) have shown a varied microbial composition compared to diabetic mice (Figures 5B,C).

**Effect of DOP on other bacterial analysis parameters**

In addition to alpha and beta diversity, several other parameters, including the flora characterization index, species composition analysis, and functional prediction analysis, were also measured. Our results suggest that diabetic mice exhibit differences compared to control mice in all these parameters. In brief, functional prediction analysis indicates a significant change in carbohydrate, lipid metabolism, and other pathways associated with T2DM in diabetic mice. Significant changes were seen in diabetic mice treated with DOP (80 mg/kg b.w) and PIO (10 µg/kg b.w) (Figure 6A). Similarly, species composition analysis reveals changes in species composition across different experimental groups (Figure 6B).

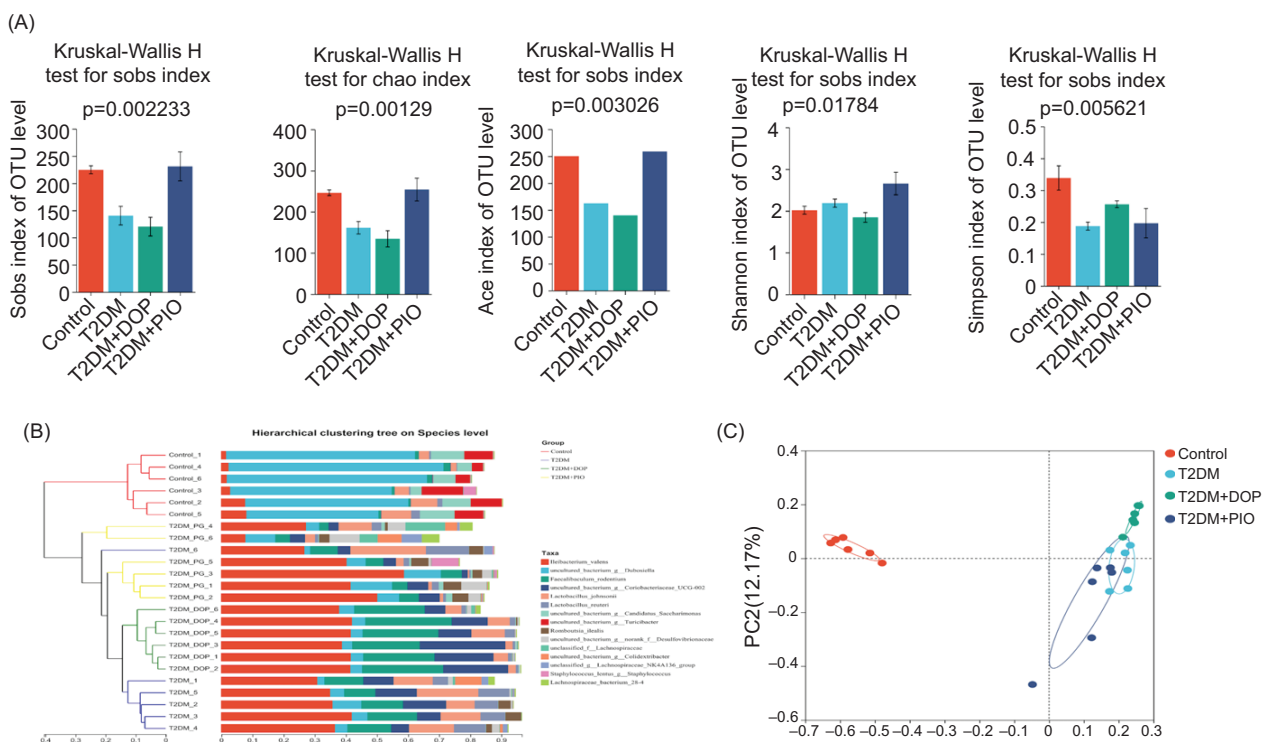


**Figure 5.** The figure depicts the changes in bacterial diversity by 16S rRNA sequencing. (A) alpha diversity-inter group differences by Kruskal–Wallis H test. (B) Beta diversity index- sample hierarchical clustering at the species level. (C) Beta diversity index-PCoA analysis on the OTU level.

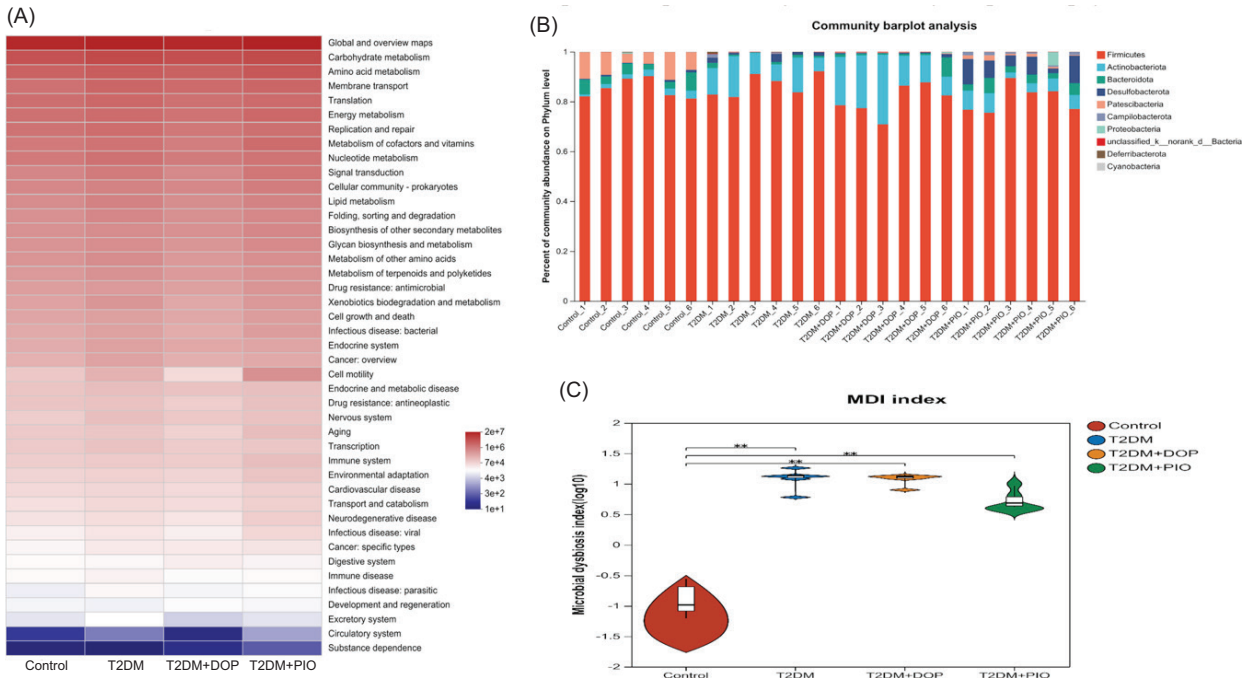


Figure 6. The figure depicts (A) function prediction analysis-PICRUSt2 functional prediction, (B) species composition analysis—community composition-phyllum level, and (C) flora characterization index-microbial dysbiosis index.

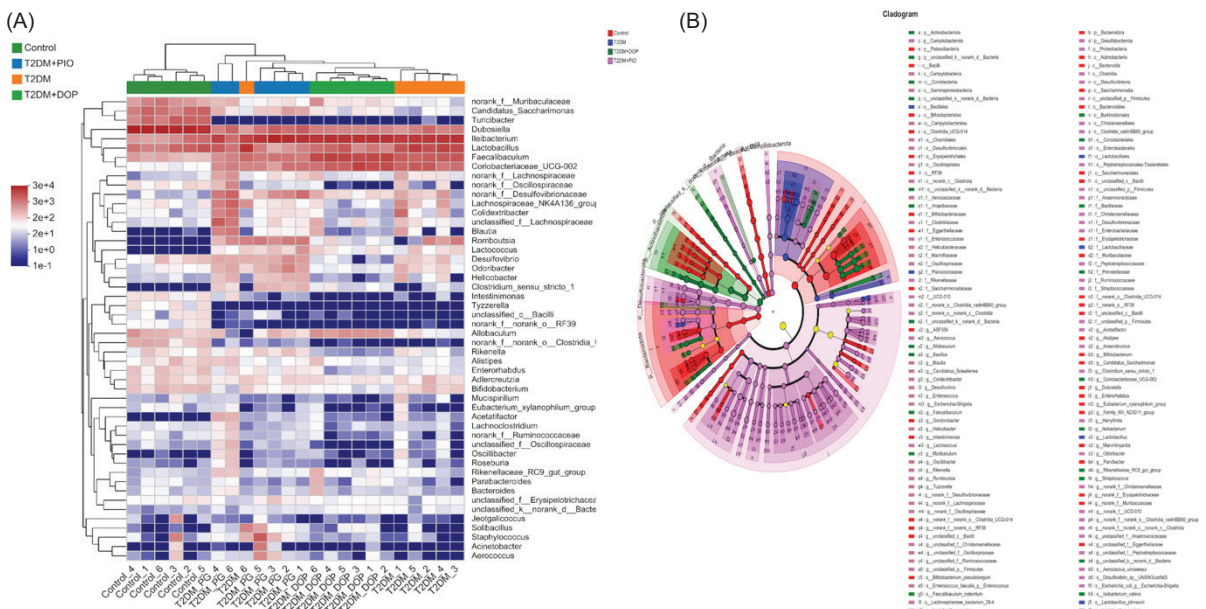


Figure 7. The figure depicts (A) species composition analysis-community heatmap on genus level and (B) multiple group difference analysis-cladogram.

Microbial dysbiosis in T2DM mice is significantly greater compared to control mice and DOP-treated mice (Figure 6C). Species composition analysis and multiple group difference analysis were mentioned in Figure 7A and Figure 7B.

## Discussion

T2DM was developed in experimental mice via a HFD and STZ. The characteristic features of HFD-/STZ-mediated T2DM are pancreatic beta-cell impairment and

insulin resistance (Dludla *et al.*, 2023). An 8-week HFD has induced a state of insulin resistance in experimental mice. In addition, a single dose of STZ (120 mg/kg b.w) has caused considerable damage to the insulin-secreting cells. This combined action reflects metabolic characteristics typical of T2DM in mice. Along with hyperglycemia, hyperlipidemia remains a key feature of T2DM because of HFD feeding (Galicia-Garcia *et al.*, 2021). A growing body of evidence suggests that the composition profile of the microbiota influences indicators of dyslipidemia and cholesterol metabolism (Ma *et al.*, 2021; Vourakis *et al.*, 2021). Hence, there is a strong association between T2DM, lipid metabolism, and gut microbes.

Hyperglycemia is a primary characteristic feature of diabetes mellitus, resulting from either reduced insulin secretion or a lack of insulin action. Diabetes mellitus affects various metabolic pathways and dysregulates various proteins and genes (Khoshnejat *et al.*, 2020). We previously reported that DOP significantly regulates hyperglycemia by altering the dysregulated insulin signaling pathway (data not shown). In addition, this time, we have studied the oral glucose tolerance and ITTs to determine the effects of HFD/STZ on developing  $\beta$ -cell damage, insulin resistance, and the capability of DOP to avert  $\beta$ -cell damage and insulin resistance. Control mice show a normal rise in glucose levels, peak at 30 minutes, and start to decline by 120 minutes. Diabetic mice exhibit a sharp rise in blood glucose, with no significant decline observed at 120 minutes, indicating their inability to manage hyperglycemia. Mice treated with DOP (80 mg/kg b.w.) have shown significant insulin sensitivity compared to diabetic mice. Similar results were seen in diabetic mice treated with PIO (10  $\mu$ g/kg b.w.) (Figure 1A). The ITT shows similar changes (Figure 1B) in the opposite direction.

Hyperglycemia and dyslipidemia are strongly associated with endothelial dysfunction of T2DM (Dhananjayan *et al.*, 2016). Insulin resistance-related increases in free fatty acids are thought to be the cause of the lipid alterations linked to diabetes mellitus (Shetty & Kumari, 2021). In our study, control mice showed normal lipid profiles in plasma and liver. Diabetic mice show an upsurge in TC, TG, LDL, and VLDL. Meanwhile, the HDL levels were drastically diminished. Diabetic mice treated with DOP have shown a significant decline in TC, TG, LDL, and VLDL levels. The levels of HDL were observed to increase in diabetic mice compared to those in nondiabetic mice. Similar results were observed in diabetic mice treated with PIO (10  $\mu$ g/kg b.w.) (Figure 2). Our results were similar to those of polysaccharide KGM, which demonstrated an antilipidemic effect in diabetic rats (Jayachandran *et al.*, 2023). Disturbances in lipid metabolism may lead to modifications in the intestinal environment, potentially resulting in internal microflora

dysbiosis (Jia *et al.*, 2021). In this context, our 16S rRNA sequencing results suggest that lipid metabolism is significantly altered in the diabetic group and improves upon treatment with DOP (Figure 6A).

In addition, changes in the histology of liver and adipose tissue because of high-fat feeding were studied using hematoxylin and Eosin and Oil red O staining. Our results suggest that control mice exhibit normal liver and adipose tissue architecture. Meanwhile, diabetic mice show significant changes in the liver, such as a fatty liver condition. Diabetic mice treated with DOP and PIO have significantly prevented the further progression of fatty liver and helped to reverse it. Similar effects of HFD were observed in the adipose tissue, and treatment with DOP significantly regulated the size of adipose tissue, similar to that of control mice. The results are similar to those of diabetic mice given PIO. Oil red O staining facilitates the precise study of lipid accumulation in various tissues. In our study, control mice show no trace of lipid accumulation with regular liver histology; in contrast, diabetic mice show a sign of fatty liver by high staining reactivity with Oil red O. Diabetic mice treated with DOP (80 mg/kg b.w) have reduced the effects of the HFD, which was visualized through its histology. Similar positive regulation was seen in diabetic mice treated with PIO. In this context, *Lycium barbarum* polysaccharide treats HFD-driven hepatic steatosis, as evidenced by Oil Red O staining (Jia *et al.*, 2016) (Figure 4).

The association between dyslipidemia, gut microbiota, and human health is strong and supported by several studies (Lei *et al.*, 2022; Zhou *et al.*, 2023). Microbial dysbiosis, resulting from disruptions in the normal microflora, is a key feature of T2DM (Zhou *et al.*, 2022). We have studied the microbial dysbiosis index, and the results suggest that a significant dysbiosis occurred between the experimental groups, indicating the effects of T2DM (Figure 6C). In general, the gut microbiota can regulate various metabolic processes and produce metabolites that have a significant impact on human health. In T2DM, gram-negative opportunistic infections that produce LPS are more common than those caused by gram-positive bacteria that produce SCFA (Ağagündüz *et al.*, 2023). One interesting study revealed that T2DM patients displayed an increased *Firmicutes/Bacteroidetes* ratio compared to normal individuals (Hung *et al.*, 2021).

In addition, T2DM patients exhibited reduced bacterial diversity compared to healthy individuals. Bacterial species such as *Faecalibacterium prausnitzii* and *Ruminococcus bromii* (involved in SCFA synthesis) are also found to be decreased in T2DM patients (Jandhyala *et al.*, 2017). Our study results indicate that diabetic mice exhibit significant changes in bacterial diversity

compared to other groups (Figure 5). Various indicators were studied, and the results suggest that diabetic mice treated with DOP (80 mg/kg b.w.) and PIO (10 µg/kg b.w.) exhibit varied responses, which could indicate their ability to alter gut microbial dysbiosis. In addition, the functional prediction analysis suggests changes in various metabolic pathways, including carbohydrate, lipid, and other pathways associated with endocrine diseases (Figure 6A).

## Conclusion

Overall, we have interpreted the effects of HFD intake in experimental mice and the relationship between T2DM, dyslipidemia, and gut microbiota. We have studied the oral glucose and insulin tolerance in different groups, and our DOP treatment results suggest its efficiency. In addition, we have evaluated the antihyperlipidemic effects of DOP using plasma and tissue lipid profiles. Further, a change in the bacterial populations in the treatment group indicates its ability to alter gut microbial dysbiosis. Meanwhile, our results highlight the potential role of DOP in the management of T2DM and also inform future directions. Precisely, importance should be given to studying the complete role of microbial metabolites such as SCFAs, which play a critical role in the host inflammation and metabolic processes. Exploring these metabolite profiles could provide a deeper understanding of the mechanistic basis for DOP's therapeutic effects. To summarize, our research suggests that DOP may play a multifaceted part in controlling hyperlipidemia, gut microbial balance, and glucose tolerance in individuals with type 2 diabetes. In addition to confirming DOP's clinical suitability, future studies in the areas mentioned earlier may aid in the development of innovative treatments for metabolic disorders that target the microbiota.

## Acknowledgment

The Shanghai Tenth People's Hospital, affiliated with Tongji University, Shanghai, provided the workspace for the research, and the authors are indebted to it.

## Data Availability

The datasets generated or analyzed during this study can be made available by the corresponding author upon reasonable request.

## Competing Interests Declaration

The authors declare no competing interests.

## Ethical Approval

Ethical permission was obtained from Shanghai Tenth People's Hospital (SHDSYY-2023-1981).

## Author Contributions

Muthukumaran Jayachandran was in charge of conceptualization, data curation, formal analysis, investigation, methodology, validation, and writing of original draft. Jia Liu did formal analysis, investigation, methodology, and writing—review and editing. Qu Shen managed project administration, resources, supervision, and writing—review and editing.

## Conflicts of Interest

None.

## Funding

This work was supported by the National Key R&D Program of China (No. 2018YFC1314101, 2016YFC1305600), National Natural Science Foundation of China (82170861, 81970677), Fundamental Research Funds for the Central Universities of Tongji University (22120190210), Clinical Research Plan of SHDC (SHDC2020CR1017B), and Shanghai Committee of Science and Technology, China (19DZ1910200, 18411951803, and 17DZ1910603).

## References

- Ağagündüz D., Icer M.A., Yesildemir O., Koçak T., Kocyyigit E., Capasso R. The roles of dietary lipids and lipidomics in gut-brain axis in type 2 diabetes mellitus. *J. Transl. Med.* 2023, 21, 240. <https://doi.org/10.1186/s12967-023-04088-5>
- Chen S., Zhou Y., Chen Y., Gu J. Fastp: An ultra-fast all-in-one FASTQ preprocessor. *Bioinformatics.* 2018, 34(17), i884–i890. <https://doi.org/10.1093/bioinformatics/bty560>
- Chong K., Chang J.K., Chuang L.M. Recent advances in the treatment of type 2 diabetes mellitus using new drug therapies. *Kaohsiung J. Med. Sci.* 2024, 40, 212–220. <https://doi.org/10.1002/kjm2.12800>
- Cunningham A.L., Stephens J.W., Harris D.A. Gut microbiota influence in type 2 diabetes mellitus (T2DM). *Gut Pathog.* 2021, 13, 50. <https://doi.org/10.1186/s13099-021-00446-0>
- Dhananjayan R., Koundinya K.S., Malati T., Kutala V.K. Endothelial dysfunction in type 2 diabetes mellitus. *Indian J. Clin. Biochem.* 2016, 31, 372–379. <https://doi.org/10.1007/s12291-015-0516-y>
- Dudla P.V., Mabhida S.E., Ziqubu K., Nkambule B.B., Mazibuko-Mbeje S.E., Hanser S., Basson A.K., Pfeiffer C., Kengne A.P.

- Pancreatic  $\beta$ -cell dysfunction in type 2 diabetes: Implications of inflammation and oxidative stress. *World J. Diab.* 2023, 14, 130–146. <https://doi.org/10.4239/wjd.v14.i3.130>
- Douglas G.M., Maffei V.J., Zaneveld J.R., Yurgel S.N., Brown J.R., Taylor C.M., Huttenhower C., Langille M.G.I. PICRUSt2 for prediction of metagenome functions. *Nat. Biotechnol.* 2020, 38(6), 685–688. <https://doi.org/10.1038/s41587-020-0548-6>
- Du Vigneaud V., Karr W.G. Carbohydrates utilization rate of disappearance of d-glucose from the blood. *J. Biol. Chem.* 1925, 66, 281–300.
- Edgar R.C. UPARSE: Highly accurate OTU sequences from microbial amplicon reads. *Nat. Methods.* 2013, 10(10), 996–998. <https://doi.org/10.1038/nmeth.2604>
- Folch J., Lees M., Sloane Stanley G.H. A simple method for the isolation and purification of total lipids from animal tissues. *J. Biol. Chem.* 1957, 226(1), 497–509.
- Galicia-García U., Benito-Vicente A., Jebari S., Larrea-Sebal A., et al. Pathophysiology of type 2 diabetes mellitus. *Int. J. Mol. Sci.* 2020, 21, 6275. <https://doi.org/10.3390/ijms21176275>
- Gevers D., Kugathasan S., Denson L.A., Vázquez-Baeza Y., Van Treuren W., Ren B., Schwager E., Knights D., Song S.J., Yassour M., et al. The treatment-naive microbiome in new-onset Crohn's disease. *Cell Host Microbe.* 2014, 15(3), 382–392. <https://doi.org/10.1016/j.chom.2014.02.005>
- Hung W.C., Hung W.W., Tsai H.J., Chang C.C., et al. The association of targeted gut microbiota with body composition in type 2 diabetes mellitus. *Int. J. Med. Sci.* 2021, 18, 511–519. <https://doi.org/10.7150/ijms.51164>
- Jandhyala S.M., Madhulika A., Deepika G., Rao G.V., et al. Altered intestinal microbiota in patients with chronic pancreatitis: Implications in diabetes and metabolic abnormalities. *Sci. Rep.* 2017, 7, 43640. <https://doi.org/10.1038/srep43640>
- Jayachandran M., Christudas S., Zheng X., Xu B. Dietary fiber konjac glucomannan exerts an antidiabetic effect via inhibiting lipid absorption and regulation of PPAR- $\gamma$  and gut microbiome. *Food Chem.* 2023, 403, 134336. <https://doi.org/10.1016/j.foodchem.2022.134336>
- Jayachandran M., Wu Z., Ganesan K., Khalid S., Chung S.M., Xu B. Isoquercetin upregulates antioxidant genes, suppresses inflammatory cytokines, and regulates the AMPK pathway in streptozotocin-induced diabetic rats. *Chem. Biol. Interact.* 2019, 303, 62–69. <https://doi.org/10.1016/j.cbi.2019.02.017>
- Jayachandran M., Zhang T., Wu Z., Liu Y., Xu B. Isoquercetin regulates SREBP-1C via the AMPK pathway in skeletal muscle to exert antihyperlipidemic and anti-inflammatory effects in STZ-induced diabetic rats. *Mol. Biol. Rep.* 2020, 47, 593–602. <https://doi.org/10.1007/s11033-019-05166-y>
- Jia L., Li W., Li J., Li Y., et al. Lycium barbarum polysaccharide attenuates high-fat diet-induced hepatic steatosis by up-regulating SIRT1 expression and deacetylase activity. *Sci. Rep.* 2016, 6, 36209. <https://doi.org/10.1038/srep36209>
- Jia X., Xu W., Zhang L., Li X., et al. Impact of gut microbiota and microbiota-related metabolites on hyperlipidemia. *Front. Cell. Infect. Microbiol.* 2021, 11, 634780. <https://doi.org/10.3389/fcimb.2021.634780>
- Kheriji N., Dakhloui T., Kamoun Rebai W., Maatoug S., et al. Prevalence and risk factors of diabetes mellitus and hypertension in North East Tunisia calling for efficient and effective actions. *Sci. Rep.* 2023, 13, 12706. <https://doi.org/10.1038/s41598-023-39197-0>
- Khoshnejat M., Kavousi K., Banaei-Moghaddam A.M., Moosavi-Movahedi A.A. Unraveling the molecular heterogeneity in type 2 diabetes: A potential subtype discovery followed by metabolic modeling. *BMC Med. Genomics* 2020, 13, 119. <https://doi.org/10.1186/s12920-020-00767-0>
- Lei L., Zhao N., Zhang L., Chen J., Liu X., Piao S. Gut microbiota is a potential goalkeeper of dyslipidemia. *Front. Endocrinol.* 2022, 13, 950826. <https://doi.org/10.3389/fendo.2022.950826>
- Li L., Yao H., Li X., Zhang Q., et al. Destiny of *Dendrobium officinale* polysaccharide after oral administration: Indigestible and nonabsorbing, ends in modulating gut microbiota. *J. Agric. Food Chem.* 2019, 67, 5968–5977. <https://doi.org/10.1021/acs.jafc.9b01489>
- Li X., Jayachandran M., Xu B. Antidiabetic effect of konjac glucomannan via insulin signaling pathway regulation in high-fat diet and streptozotocin-induced diabetic rats. *Food Res. Int.* 2021, 149, 110664. <https://doi.org/10.1016/j.foodres.2021.110664>
- Liu C., Zhao D., Ma W., Guo Y., et al. Denitrifying sulfide removal process on high-salinity wastewaters in the presence of *Halomonas* sp. *Appl. Microbiol. Biotechnol.* 2016, 100, 1421–1426.
- Liu H., Xing Y., Wang Y., Ren X., et al. *Dendrobium officinale* polysaccharide prevents diabetes via the regulation of gut microbiota in prediabetic mice. *Foods* 2023, 12, 2310. <https://doi.org/10.3390/foods12122310>
- Liu Y., Yang L., Zhang Y., Liu X., et al. *Dendrobium officinale* polysaccharide ameliorates diabetic hepatic glucose metabolism via glucagon-mediated signaling pathways and modifying liver-glycogen structure. *J. Ethnopharmacol.* 2020, 248, 112308. <https://doi.org/10.1016/j.jep.2019.112308>
- Ma Y., Sun Y., Sun L., Liu X., et al. Effects of gut microbiota and fatty acid metabolism on dyslipidemia following weight-loss diets in women: Results from a randomized controlled trial. *Clin. Nutr.* 2021, 40, 5511–5520. <https://doi.org/10.1016/j.clnu.2021.09.021>
- Magoc T., Salzberg S.L. FLASH: Fast length adjustment of short reads to improve genome assemblies. *Bioinformatics.* 2011, 27(21), 2957–2963. <https://doi.org/10.1093/bioinformatics/btr507>
- Quast C., Pruesse E., Yilmaz P., Gerken J., Schweer T., Yarza P., Peplies J., Glöckner F.O. The SILVA ribosomal RNA gene database project: Improved data processing and web-based tools. *Nucleic Acids Res.* 2013, 41(D1), D590–D596. <https://doi.org/10.1093/nar/gks1219>
- Ruze R., Liu T., Zou X., Song J., et al. Obesity and type 2 diabetes mellitus: Connections in epidemiology, pathogenesis, and treatments. *Front. Endocrinol.* 2023, 14, 1161521. <https://doi.org/10.3389/fendo.2023.1161521>
- Schloss P.D., Westcott S.L., Ryabin T., Hall J.R., Hartmann M., Hollister E.B., Lesniewski R.A., Oakley B.B., Parks D.H., Robinson C.J., et al. Introducing mothur: Open-source, platform-independent, community-supported software for

- describing and comparing microbial communities. *Appl. Environ. Microbiol.* 2009, 75(23), 7537–7541. <https://doi.org/10.1128/AEM.01541-09>
- Shetty S.S., Kumari S. Fatty acids and their role in type-2 diabetes (Review). *Exp. Ther. Med.* 2021, 22, 706. <https://doi.org/10.3892/etm.2021.10138>
- Sun H., Saeedi P., Karuranga S., Pinkepank M., Ogurtsova K., et al. Erratum to “IDF diabetes atlas: Global, regional and country-level diabetes prevalence estimates for 2021 and projections for 2045” [*Diabetes Res. Clin. Pract.* 183 (2022) 109119]. *Diabetes Res. Clin. Pract.* 2023, 204, 110945. <https://doi.org/10.1016/j.diabres.2023.110945>
- Vourakis M., Mayer G., Rousseau G. The role of gut microbiota on cholesterol metabolism in atherosclerosis. *Int. J. Mol. Sci.* 2021, 22, 8074. <https://doi.org/10.3390/ijms22158074>
- Wang P., Liu Y., Zhang T., Yin C., et al. Effects of root extract of *Morinda officinalis* in mice with high-fat-diet/streptozotocin-induced diabetes and C2C12 myoblast differentiation. *ACS Omega* 2021, 6, 26959–26968.
- Wang Q., Garrity G.M., Tiedje J.M., Cole J.R. Naive Bayesian classifier for rapid assignment of rRNA sequences into the new bacterial taxonomy. *Appl. Environ. Microbiol.* 2007, 73(16), 5261–5267. <https://doi.org/10.1128/AEM.00062-07>
- Wondmkun Y.T. Obesity, Insulin resistance, and type 2 diabetes: Associations and therapeutic implications. *Diabetes Metab. Syndr. Obes. Targets Ther.* 2020, 13, 3611–3616. <https://doi.org/10.2147/DMSO.S275898>
- Wu W., Zhao Z., Zhang D., et al. Structure, health benefits, mechanisms, and gut microbiota of *Dendrobium officinale* polysaccharides: A review. *Nutrients* 2023, 15, 4901. <https://doi.org/10.3390/nu15234901>
- Xu X., Zhang C., Wang N., Xu Y., Tang G., Xu L., Feng Y. Bioactivities and mechanism of actions of *dendrobium officinale*: A comprehensive Review. *Oxid. Med. Cell. Longev.* 2022, 2022, 6293355. <https://doi.org/10.1155/2022/6293355>
- Zhao Y., Jayachandran M., Xu B. In vivo antioxidant and anti-inflammatory effects of soluble dietary fiber Konjac glucomannan in type-2 diabetic rats. *Int. J. Biol. Macromol.* 2020, 159, 1186–1196. <https://doi.org/10.1016/j.ijbiomac.2020.05.105>
- Zhou X., Lian P., Liu H., Wang Y., Zhou M., Feng Z. Causal associations between gut microbiota and different types of dyslipidemia: A two-sample mendelian randomization study. *Nutrients* 2023, 15, 4445. <https://doi.org/10.3390/nu15204445>
- Zhou Z., Sun B., Yu D., Zhu C. Gut microbiota: An important player in type 2 diabetes mellitus. *Front. Cell. Infect. Microbiol.* 2022, 12, 834485. <https://doi.org/10.3389/fcimb.2022.834485>